WEDGE-SHAPED, LARGE-APERTURE, DIPOLE MAGNET DESIGNS FOR THE JEFFERSON LAB FEL UPGRADE

D. Newsham, A. Smirnov, Y. Luo, D. Yu
DULY Research Inc., Rancho Palos Verdes, CA 90275
G. Biallas*, JLAB, Newport News, VA*

Abstract

Two types of dipole magnets were simulated and designed for the Thomas Jefferson National Accelerator Facility FEL upgrade. The magnets are to operate in series with a common power supply, and to provide ~0.01% accuracy of the field amplitude *and* field integral over a large aperture. The wedged magnets have quite different angles and effective length-to-aperture aspect ratios. The most difficult design problem was to provide high field quality in the magnet having a small aspect ratio ~2.7 and a 20° wedge angle. A design was developed which enabled small adjustments to be made before and after installation of the magnets. Trim coils, shims, and side sliders in the field clamps were introduced to compensate field gradients, non-uniformities, and parasitic fringe field effects. A number of design and adjustment issues are discussed.

INTRODUCTION

The upgrade project of a CW 1-kW infrared free-electron laser at the Thomas Jefferson National Accelerator Facility (JLab) [1] aims to produce higher power IR and shorter wavelength radiation, and includes two families of new extraction/injection dipole focusing magnets of different geometries (see Table 1).

Table 1. Specifications of GU and GV dipole magnets

Magnet family	GU	GV
Maximum beam energy E, MeV	160	11
Wedge angle α, degrees	4.87	20
Bend radius R, m	9.6	0.6
Maximum induction B, Tesla	0.0612	0.0612
Effective length L, mm	435	208
Vertical magnetic gap G, mm	76.2	≥76.2
Horizon. good field region, mm	≥76.2	≥76.2
Field non-uniformity ΔB/B along the horizon. Line of symmetry), %	±0.01	±0.01
Field integral non-uniformity over good field region ΔIB/IB, %	±0.01	±0.01

The need for high field quality ($\sim 10^{-4}$) is driven by the requirement to suppress two main spurious effects: steering and focusing. Both are important for transport of a low-emittance beam having a large spot size and a halo (at maximum power). Compact design of the beam lattice requires usage of field clamps limiting the extent of the stray fields. An additional, important requirement is minimization of beam quality degradation caused by AC ripples. It implies the same current in both magnets, which are connected in series with a common power supply. Field non-uniformity is considered at the vertical plane of symmetry. Non-uniformity of the field integral is defined as the relative deviation with respect to an ideal model having the same effective length, wedge angle and uniform field B over the hard-edge trapezoidal volume. Field integral is defined along a straight line (theoretically for infinite particle energy) tangent to the beam centroid trajectory.

A 3D code Radia [2] was used in design simulations. In both models of the GU and GV magnets, equal angular dimension of each trapezoidal sub-segment was chosen in a fine mesh (up to 1 GB of RAM). Post-processing included trajectory analysis with calculation of end-field roll-off integral K_1 as defined in ref. [5], and focal length F.

GU MAGNET DESIGN

The GU magnet differs from an earlier prototype [3] in its wedged shape and field clamps. Some new design elements are the use of a Purcell gap, field clamps with adjustable longitudinal position, and non-magnetic gap. The Purcell gap consists of two thin layers: non-magnetic material and material with extremely high permeability up to 500,000 (see, e.g., CO-NETIC AA [4]). It was applied effectively for larger rectangular magnets with measured field flattening effect better than 5 times [5].

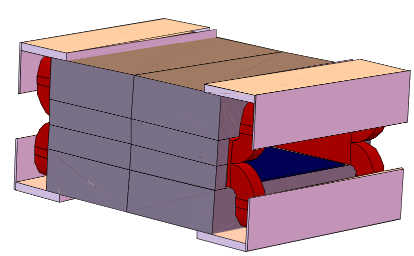

Figure 1: Radia schematic view of the GU magnet.

3D Radia modeling initially revealed significant numerical instability and slow convergence. These severe issues were caused by a high aspect ratio of the μ-metal plate (~250) with extremely high permeability. The problem was solved with a procedure of multi-parametric optimization of subdivision of the main objects.

During minimization of the field inhomogeneity we defined optimal dimensions of the μ-metal plate and field clamp configuration. The wave-like behavior of the field quality shown in Fig. 2 reflects in part the numerical effect of residual relaxation related to the large interaction

0-7803-7739-9

matrix having many nearly equal elements. With some combinations of the segmentation parameters and number of elements, the curves can be smoothed. Fig. 3 illustrates the sensitivity to the horizontal displacement of the clamps with respect to vertical plane of symmetry.

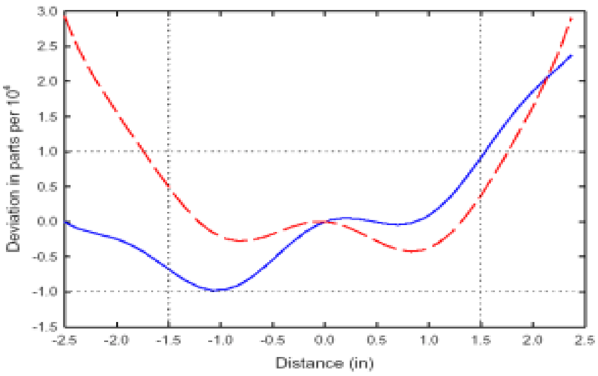

Figure 2: Relative deviation of the field integral (solid curve) and field (dashed) for the GU magnet.

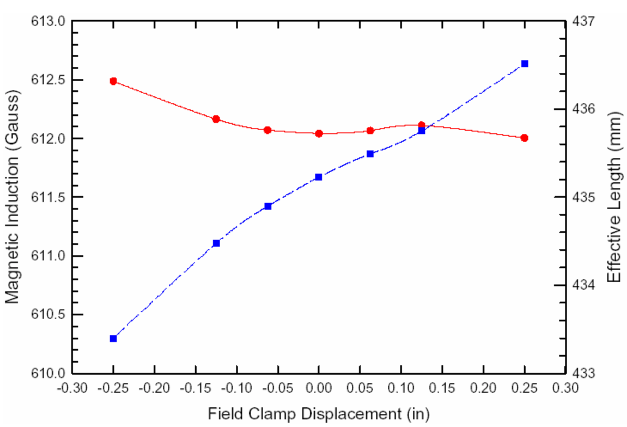

Figure 3: Sensitivity of the field (solid curve) and effective length (dashed) to symmetric shift of the clamps for the GU magnet.

GV MAGNET DESIGN

In designing the GV magnet two additional issues were addressed: suppression of the field gradient caused by a large wedge angle, and achievement of the parameters specified in Table 1 along with the same value of current found for GU magnet (2.1 kA). Unlike most conventional magnets, the GV magnet has a shorter length (with respect to the transverse gap) and a bigger wedge angle. It causes large non-uniformity of both the field and field integral, exceeding the nominal by more than one order. Also, unlike GU and other magnet designs [3,5,6], the Purcell gap turned out to be ineffective: the GV magnet is dominated by 3D effects of non-uniform fringe-field at shorter lengths. The sensitivity of the effective length of the GV magnet to the shift of the field clamps is almost twice as high as that for the GU magnet.

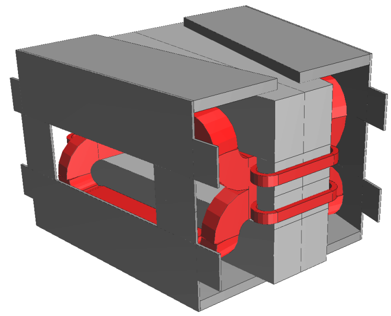

Figure 4: Schematic view of the GV magnetic design.

To provide field homogeneity in the GV design (see Fig. 4), three sets of additional elements were introduced. Trim coils on each of the return legs of the yoke suppress the field gradient. The coils on the opposite legs have the same current to provide increased magnetic flux for the smaller leg and decreased flux for the bigger one. Side sliders at the clamps provide adjustability of the field integral profile with tunable magnetic shortcut at the periphery of the window-framed aperture in the clamps. Finally, a set of shims, *i.e.* small pieces of μ-metal, are placed along the median line between the internal surface of horizontal clamps and the conductor. Thus trim coils provide the first-order (gradient) compensation of the field and field integral, μ-metal pieces provide the second-order compensation, and side sliders provide non-linear corrections for the field integral. In the mechanical design of the GU and GV magnets, we introduced an additional degree of freedom enabling compensation of the remnant slope of the field integral by a small angular shift of the clamps with respect to the yoke.

To provide the field required with the same current as it was computed for the GU magnet, we found numerically the optimized value of an enlarged vertical magnetic gap, along with other parameters of this final design. The GV magnet field quality in the median plane is depicted in Fig. 5.

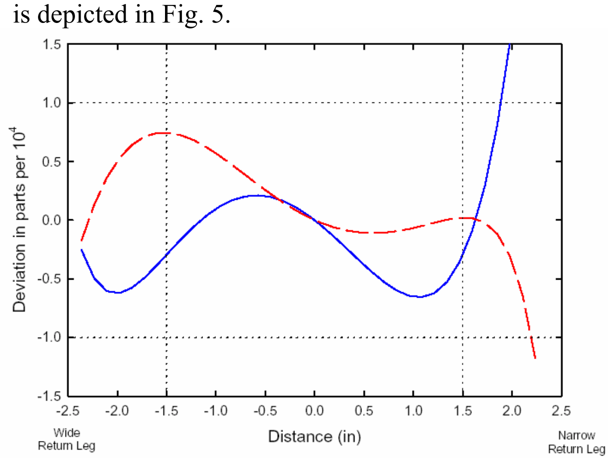

Figure 5: Relative deviation of the field (solid curve) and field integral (dashed) for the GV magnet.

Table 2: a) Computed sensitivities of the GV magnet parameters to the main adjustments

1GB-RAM Model with different conductor configuration	Not smoothed	Smoothed
Effective length to the symmetrical shift of all clamps along the trajectory, $\Delta L_{eff} / \Delta S_{clamp}$	0.295	0.271
Relative gradient of the field related to the relative trim coil current, $\Delta B / (\Delta x B_o) / \Delta I_{trim} / I_o$, averaged over central part of the good area, (%/m)	59	67.2
Gradient of relative field Integral to the angular position of the field clamp, $\left[\Delta \int Bdz / (\Delta x B_o L_{eff})\right] / \Delta \varphi_{clamp}$, averaged over the linearized part of good area, (%/m-mrad)	0.098	0.13

b) Computed optimal adjustments to provide specification parameters

Overlap of horiz. part of the field clamp with the body magnet along the central axis, (inches)	1.21-1.22	1.23-1.24
Trim coil current related to the main current, I_{trim} / I_o, (%)	4.99-5.1	4.9-5.1
Angular clamp position, (mrad)	-7.36	-5.1-2.77
Shift of wider-side slider towards the axis (from the nominal in mechanical drawings), (mm)	0-5	0

We studied the sensitivity of the main magnet parameters to the aforementioned tuning means. The results of this study are given in the Table 2 and implemented in the tolerances of the mechanical design. We noticed also a high sensitivity to the shape of the bent conductor parts (twisted arc-arc and bar-arc conjunctions).

CONCLUSION

Extensive studies of magnetic design demonstrated feasibility of the specified requirements. On the basis of these results, mechanical design of both magnets was made. The GU and GV magnets were manufactured and tested at Jlab GV magnet field measurements demonstrated ±0.01% deviation for the field, and ±0.02% for the field integral [7] over the good area. Note, only trim coils were used to adjust the field. In the real design, the field amplitude, field uniformity, and the effective length are affected by holes (for bolts, alignment pins, *etc.*) in the yoke and clamps, real shape of the main coil (especially conductor conjunctions), geometric tolerances and imperfections of magnetic materials. These features cannot be reproduced accurately in the numerical model, which has inherent numerical inaccuracy as well.

The key underlying concept of the cost-saving design of the GU and GV magnets is to provide flexibility with a number of adjustable elements. These elements include: field clamp longitudinal and angular positions, non-magnetic gap in the field clamps (GU only), side sliders in the clamps and μ-metal shims (GV only), trim coils and their adjustable current (GV only), and an adjustable common power supply.

The field and current differences between the GU and GV magnets can easily be compensated with a low-current (~a few Amperes), variable shunting resistors connected in parallel to main coils of the magnets.

REFERENCES

[1] D. Douglas *et al*., in Proc. of the 2001 Part. Acc. Conf., Chicago (2001) 249.

[2] P. Elleaume *et al*., Proc. of the IEEE Particle Accelerator Conference, May 1997, Vancouver, BC, Canada, p. 3509.

[3] G. Biallas *et al*., Proc. of the 1999 Particle Accelerator Conference, New York, March-April 1999, p. 3306.

[4] http://magnetic-shield.com/graphics/perm-graph.jpg

[5] J. Karn *et al.,* Proc. of the IEEE Particle Accelerator Conference, May 1997, Vancouver, BC, Canada, p. 3333

[6] G. Biallas *et al*., in Proc. of the IEEE Particle Accelerator Conference, New York, March-April 1999, p. 3312

[7] G. Biallas *et al*., these proceedings.